Numerical study of the human phonation process by the Finite Element Method

S. Zörner[1,2], M. Kaltenbacher[1], Gerhard Link[2], Reinhard Lerch[2], Michael Döllinger[3]

[1] *Alps-Adriatic University of Klagenfurt, Chair of Applied Mechatronics*

[2] *Universität Erlangen-Nürnberg, Depart. of Sensor Technology,*

[3] *Universität Erlangen-Nürnberg, Depart. of Phoniatrics & Pediatric*

Introduction

The basis of the human phonation process is given by the complex interaction of air flow in the larynx together with the structural mechanics of the vocal folds. The air flows through the larynx thereby acting on the vocal folds and forcing them to vibrate. These vibrations in turn influences the fluid flow. The acoustic sound is generated due to the fluid flow and the vibration of the vocal folds To get a better insight into the human phonation process we present a numerical method that is capable to fully compute the fluid-solid-acoustic interaction. This gives the possibility to analyse the effect on the fluid field, the movement of the vocal folds and the generated sound, e.g. for different geometric shapes of the vocal folds.

Physical fields

Figure 1 provides an overview of our computational scheme. In the following, we will shortly describe the induced physical fields and their interactions. The arising partial differential equations (PDEs) are all solved by applying the Finite-Element method (FEM). For a detailed discussion we refer to [5, 4].

Fluid mechanics

Due to the fact, that for the considered application the Mach number is smaller than 0.3, an incompressible flow may be assumed. Thereby the governing set of partial differential equations is given by the momentum and mass conservation

$$\rho\frac{\partial\vec{v}}{\partial t}+\rho(\vec{v}\cdot\nabla)\vec{v}+\nabla p-\mu\Delta\vec{v}=0\,, \tag{1}$$

$$\nabla\cdot\vec{v}=0\,, \tag{2}$$

with $\vec{v}$ the flow velocity, ρ the fluid density, p the hydrodynamic pressure and μ the dynamic viscosity. Since the moving of the vocal folds constantly change the position of the fluid-solid interface the Arbitrary-Lagrangian-Eulerian (ALE) approach has been utilised (for details see [1, 2]).

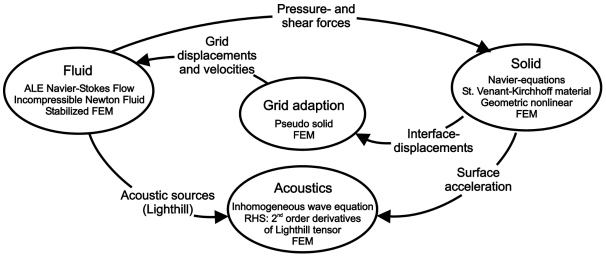

Figure 1: Fluid-solid-acoustic interaction: Navier-Stokes equation, Navier's equation, wave equation.

Solid mechanics

The vibrations of the vocal folds are modelled by Navier's equation

$$\nabla\cdot\sigma_{\mathrm{s}}=\frac{1}{\rho_{\mathrm{s}}}\frac{\partial^2}{\partial t^2}\vec{u}\,, \tag{3}$$

where σ_{s} denotes the Cauchy stress tensor, ρ_{s} the density of the solid and $\vec{u}$ the mechanical displacement. Introducing the tensor of elasticity $[c]$ and tensor of linear strain $[S]$, allows us to express Hook's law by

$$\sigma_{\mathrm{s}}=[c][S] \tag{4}$$

and the linear strain-displacement by

$$[S]=\nabla^{\mathrm{sym}}\vec{u}\,. \tag{5}$$

Substituting (4) and (5) into (3) results in the final PDE for linear elasticity

$$\mathcal{B}^T[c]\mathcal{B}\vec{u}=\frac{1}{\rho_{\mathrm{s}}}\frac{\partial^2}{\partial t^2}\vec{u} \tag{6}$$

with the differential operator $\mathcal{B}$ which results in the 2d plane case as

$$\mathcal{B}=\begin{pmatrix}\frac{\partial}{\partial x} & 0\\ 0 & \frac{\partial}{\partial y}\\ \frac{\partial}{\partial y} & \frac{\partial}{\partial x}\end{pmatrix}.$$

Fluid-solid interaction

Along the common interface Γ_{fs} all nodes need to coincide for both fields given by

$$\vec{x}_{\mathrm{f}}=\vec{x}_{\mathrm{s}}\qquad\text{on }\Gamma_{\mathrm{fs}}\,. \tag{7}$$

It is assumed that the fluid adheres at the body resulting in the following condition

$$\vec{v}=\frac{\partial}{\partial t}\vec{u}\qquad\text{on }\Gamma_{fs}\,. \tag{8}$$

This implies that fluid velocity and the first time derivative of the solid displacement are identical. For solid mechanics the boundary condition is given by an inhomogeneous Neumann condition

$$[\sigma_{\mathrm{s}}]\cdot\vec{n}=[\sigma_{\mathrm{f}}]\cdot\vec{n}\qquad\text{on }\Gamma_{\mathrm{fs}} \tag{9}$$

describing the equivalent of fluid stress $[\sigma_{\mathrm{f}}]$ and solid stress $[\sigma_{\mathrm{s}}]$ in normal direction $\vec{n}$. The fluid stresses can be written

explicitly by the hydrodynamic pressure p and fluid velocity $\vec{v}$ as

$$\vec{\sigma}_\mathrm{f} = \underbrace{\rho_\mathrm{f} \int_{\Gamma_\mathrm{fs}} -pI \cdot \vec{n}\, \mathrm{d}x}_{\text{pressure}} + \underbrace{\int_{\Gamma_{fs}} \mu \left(\nabla\vec{v} + (\nabla\vec{v})^T \cdot \vec{n}\right) \mathrm{d}x}_{\text{shear}} . \quad (10)$$

Having Dirichlet boundary condition for the fluid and Neumann boundary conditions for the solid mechanics the fluid-solid interaction is also called Dirichlet-to-Neumann problem.

Acoustic field

With the equation of continuity and momentum, Lighthill's equation in pressure form is derived (for details, cf. [3])

$$\frac{1}{c^2}\frac{\partial^2 p'}{\partial t^2} - \Delta p' = \nabla \cdot (\nabla \cdot \mathbf{T}) , \quad (11)$$

with c the speed of sound and $\mathbf{T}$ the Lighthill tensor

$$T_{ij} = \underbrace{\rho_f v_i v_j}_{\text{Reynolds stress}} + \underbrace{\tau_{ij}}_{\text{Viscous stress}} + \underbrace{[(p-p_0) - c^2(\rho_f - \rho_0)]\delta_{ij}}_{\text{Heat conduction}} . \quad (12)$$

Thereby, p_0 denotes the mean pressure, ρ_f the fluid density and ρ_0 its mean density. It is assumed that no heat conduction takes place and the viscous stress may be neglected [3]. Therefore an approximation of (12) can be given by

$$T_{ij} \approx \rho_\mathrm{f} v_i v_j . \quad (13)$$

Vibrational induced sound is also included, which is a surface coupled phenomenon. The vibration of the solid causes wave propagation into the fluid. Thereby, along the common interface Γ_fs the mechanical surface velocity and the acoustic particle velocity $\vec{v}_\mathrm{a}$ need to be identical in normal direction

$$\frac{\partial}{\partial t}\vec{u} \cdot \vec{n} = \vec{v}_a \cdot \vec{n} \qquad \text{on } \Gamma_\mathrm{fs} . \quad (14)$$

With the relation linearised Euler equation

$$\frac{\partial}{\partial t}\vec{v}_a \cdot \vec{n} = -\frac{1}{\rho_\mathrm{f}}\frac{\partial}{\partial n}p' \quad (15)$$

the source terms in pressure formulation is

$$\frac{\partial}{\partial n}p' = -\rho_\mathrm{f}\frac{\partial^2}{\partial t^2}\vec{u} \cdot \vec{n} \qquad \text{on } \Gamma_\mathrm{fs} . \quad (16)$$

For the considered case we assume, that there is no back reaction of the acoustic onto the solid.

Simulation setup

The geometric setup of the vocal folds have been adopted from the model presented in [6] and inserted into our computational domain which is shown in Figure 2. The finite-element mesh consists of second order quadrilateral elements with about 22.000 elements for the fluid/acoustic domain and approx. 3.000 elements for the mechanical domain. This discretisation results in 226.074 Defrees-Of-Freedom (DOFs) for the fluid field, 18.380 DOFs for the solid and 69.441 DOFs for the acoustic field.

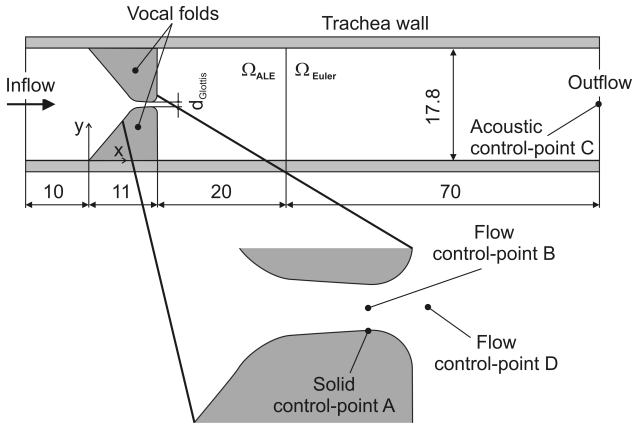

Figure 2: Simulation setup of the human larynx (distances are given in mm).

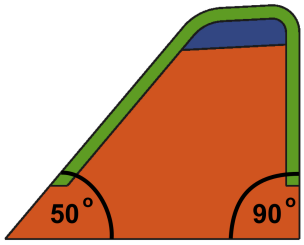

Figure 3: Vocal fold model divided into subregion with each having different material parameters.

As can be seen in Figure 3 the vocal fold model presented in [6] was additional extended by dividing the vocal folds in three different layers each having different material parameters. The elasticity modulus of body, cover and ligament are chosen 40, 10, and 100 kPa. The Poisson number is set to 0.4 for all materials.
The simplification to the 2d plane setup has been affirmed with 3d simulations [5].

Results

In order to investigate the movement of the vocal folds a pressure drop of 500 Pa from in- to outflow was chosen. The simulation shows the different stages of the vocal fold movement which is depicted in Figure 4. From the starting point (a) the vocal fold move towards each other and the glottis becomes convergent (*b*). Thereupon the vocal fold move towards the outflow, opening the glottis and giving a divergent shape (*d*). The glottis converge again (*e* and *f*) starting the next cycle.

The displacement of the vocal folds and the sound signal where compared with different vocal fold forms, which is depicted in Figure 5. At first an Eigenfrequency analysis was made, with the results given in Table 1. This showed that for thicker vocal folds the first Eigenfrequency is higher than for the thinner ones. These first Eigenfrequencies are identical

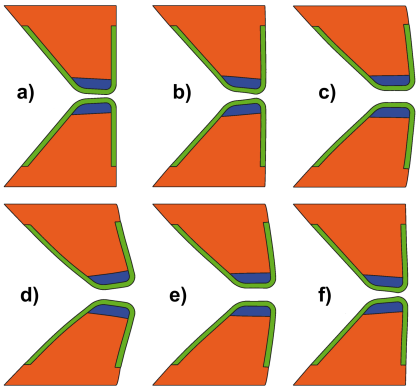

Figure 4: Computed deformation cycle of the vocal folds.

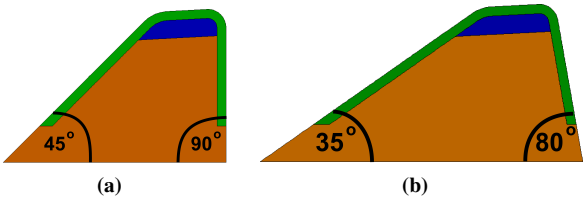

Figure 5: Variation of vocal fold form.

to the main frequency of the displacements of the vocal folds in the fully coupled transient simulation. A FFT of the vocal fold oscillation in fluid flow direction is given in Figure 6.

vocal fold angles	1^{st} Eigenfrequency
50° front 90° back	103 Hz
45° front 90° back	107 Hz
35° front 80° back	123 Hz

Table 1: Eigenfrequency of vocal folds with different shape.

Furthermore, the thick vocal fold as shown in Figure 5b shows a much smaller displacement than the other setups which is explained by its width. Due to this fact the glottis opening stays small, which results in higher velocities in the glottis area due to Bernoulli's principle. Higher fluid velocity results in greater acoustic sources than in the other setups, hence the acoustic pressure is higher, which can be observed in Figure 7.

Figure 6 and Figure 7 show that the main frequencies of the mechanical displacements and the acoustic pressure, are not the same. This comes from the fact, that in our present simulation the vocal folds do not fully close which would result in a pulsating airflow which give a distinct sound at the same frequency.

Conclusion

A computational scheme has been presented to simulate the human phonation process with all relevant physical fields. Realistic self-sustained vocal fold oscillation, which where induced by airflow through the larynx have been presented. Furthermore, an Eigenfrequency analysis of different vocal fold forms showed that the first Eigenfrequency is identical to the vibration frequency in a transient setup.
The generated sound showed dominant peaks in the frequency domain, which vary with the vocal fold form.

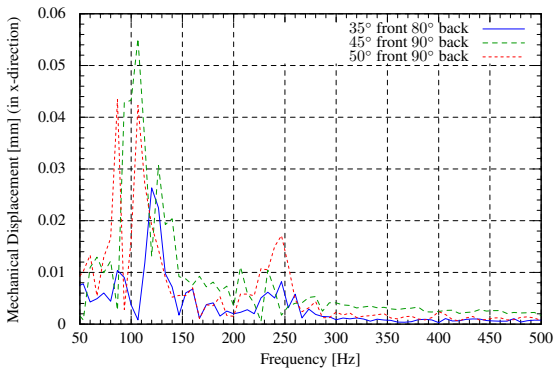

Figure 6: Displacement frequency for different sets of vocal folds.

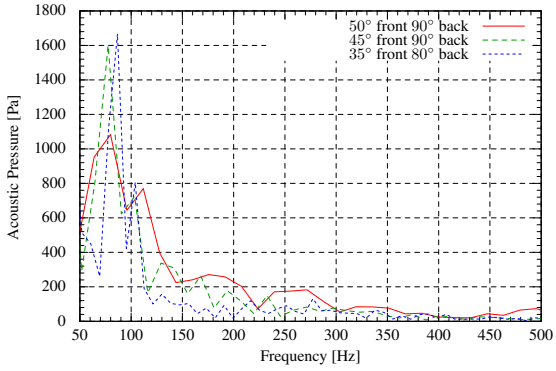

Figure 7: Displacement-frequency curve for different sets of vocal folds.

Acknowledgements

Funding by the German Research Foundation (Deutsche Forschungsgemeinschaft, DFG) is gratefully acknowledged.

References

[1] T. Belytschko, W.K. Liu, and B. Moran. *Nonlinear Finite Elements for Continua and Structures*. J. Wiley & Sons Ltd, Chichester, 2000.

[2] J. Donea and A. Huerta. *Finite element methods for flow problems*. Wiley, 2003.

[3] M. J. Lighthill. On sound generated aerodynamically I. General theory. *Proceedings of the Royal Society of London*, 1951.

[4] G. Link, M. Kaltenbacher, M. Breuer, and M Döllinger. A 2d finite-element scheme for fluid-solid-acoustic interactions and its application to human phonation. *Computer Methods in Applied Mechanics and Engineering*, 2009. (submitted).

[5] Gerhard Link. *A Finite Element Scheme for Fluid-Solid-Acoustics Interactions and its Application to Human Phonation*. PhD thesis, Der Technischen Fakultät der Universität Erlangen-Nürnberg, 2008.

[6] S.L. Thomson, L. Mongeau, and S.H. Frankel. Physical and numerical flow-excited vocal fold models. In *3rd International Workshop MAVEBA*, pages 147–150.

Firenze University Press, 2003. ISBN 88-8453-154-3.